MS-No.: esd-2016-40
Version: Revision
Title: On determining the point of no return in climate change
Author(s): van Zalinge, Feng and Dijkstra

Point by point reply to reviewer #1

November 24, 2016

We thank the reviewer for the useful comments on the manuscript and a point-by-point reply follows below. The aim of the manuscript is to introduce the new methodology combining stochastic viability theory, linear response theory and economic modeling to address the concept of the Point of no Return π_t. We indeed realize that the models used are only illustrative of the methodology and not aimed to provide a realistic estimate of π_t. Although this was mentioned in the original manuscript (in the discussion), it will be mentioned much more explicitly in the revised manuscript.

1: Climate system not well behaved
Reply:

In section 3 of the paper we show (using a simplified energy balance model (EBM)) that in principle tipping points can be taken into account to determine π_t once the PDF of the GMST can be computed (as can be done for the EBM). However, when linear response theory is used to compute PDFs, such as in section 4 for the PLASIM, indeed tipping behavior cannot be captured. This will now be mentioned more explicitly in the revised discussion of the paper.

2. GMST normally distributed
Reply:

This is indeed an assumption limiting the applicability of the methodology. The PDFs of PLASIM are approximately Gaussian but this is not expected to hold for any climate model and in particular when transitions do occur, PDFs are not Gaussian. Again this will be mentioned in the revised discussion.

3. Optimal mitigation scenario
Reply:

We do agree that this view on the economic costs of mitigation is simplified although we directly use results from the POLES model regarding the stabilization scenarios (Edenhofer et al. 2010). However, by the recommendation of both reviewers, we will delete section 4.3 of the paper, but we will mention the possibility of determining optimal mitigation scenarios in the revised discussion.

MS-No.: esd-2016-40
Version: Revision
Title: On determining the point of no return in climate change
Author(s): van Zalinge, Feng and Dijkstra

Point by point reply to reviewer #2

November 24, 2016

We thank the reviewer for the detailed report and the very useful comments on the manuscript. A point-by-point reply follows below, where we refer to each section of the report.

4. Recommendation
Reply:

The aim of the paper is to introduce a novel methodology, combining stochastic viability theory, linear response theory and economic modeling to address the concept of the point of no return π_t. Indeed, the models employed (even the PLASIM), the mitigation scenarios and the cost function are highly idealized. However, they are used here to illustrate the methodology and not to provide a realistic estimate of π_t. Although this was mentioned in the original manuscript (in the discussion), we agree that we should provide a much more critical discussion and we will do so in the revised paper. Determining the point of no return in a realistic setting is the next step on which we are currently working and is basically a new paper.

2.4 The model for and analysis of the cost function
Reply:

Also based on the recommendation of reviewer #1, the original section 4.3 will be deleted in the revised paper. Instead we will mention the possibility of determining optimal mitigation scenarios in the revised discussion.

2.3 The energy balance model
Reply:

This model is indeed constructed to illustrate the methodology in the presence of a saddle-node bifurcation. We think that it serves this purpose, without claiming to be realistic here (which is questionable anyway with these type of models). In the revised version, this will be explicitly mentioned.

2.2 Science-fiction scenarios
Reply:

We agree but this is an additional detail which is not needed to illustrate the concept of the point of no return and the methodology to determine it.

However, in the revised section 4.2, we will discuss the effect of the value of the e-folding time scale (for the PLASIM) on the results.

2.1 How to use simplified models
Reply:

Our opinion is that models should always be targeted to the question which is asked. Idealized models can be used when answering questions on mechanisms and illustrating methodology, but it is questionable whether such simplified models can determine relations between relevant observables (here radiative forcing and the global mean temperature). Anyway, our motivation here is to use these models only to illustrate the methodology and concepts and in that respect this is justified.

1. General comments
Reply:

The only remaining issue is the fact that the point of no return can indeed occur before the climate becomes non-viable due to the delay of the carbon cycle response. We will address this issue in the revised discussion.

3. Some minor points
Reply:

Page 6, lines 163–167: Suggestion will be followed and the value of σ^2 will be mentioned.

Figure 3: More information will be provided to explain the results of this figure.

Page 10, lines 261–263: We will add a paragraph to explain this difference.

Page 15, line 384: We were not aware of the Rypdal (2015) paper where this suggestion is made. We will compare this approach with the one based on linear response theory and add the results in the revised paper.

Manuscript prepared for Earth Syst. Dynam.
with version 2015/04/24 7.83 Copernicus papers of the LaTeX class copernicus.cls.
Date: 18 March 2017

On determining the Point of no Return in Climate Change

Brenda C. van Zalinge[1], Qing Yi Feng[1], Matthias Aengenheyster[1], and Henk A. Dijkstra[1]

[1]Institute for Marine and Atmospheric Research Utrecht, Department of Physics, Utrecht University, Utrecht, the Netherlands

Correspondence to: Qing Yi Feng (Q.Feng@uu.nl)

Abstract. Earth's Global Mean Surface Temperature (GMST) has increased by about 1.0°C over the period 1880-2015. One of the main causes is thought to be the increase in atmospheric greenhouse gases (GHGs). If GHG emissions are not substantially decreased, several studies indicate there will be a dangerous anthropogenic interference (DAI) with climate by the end of this century. However, there is no good quantitative measure to determine when it is ~~"too late"~~ 'too late' to start reducing GHGs in order to avoid DAI. In this study, we develop a method for determining a so-called Point of No Return (PNR) for several GHG emission ~~scenario's~~scenarios. The method is based on a combination of stochastic viability theory and uses linear response theory to estimate the probability density function of the GMST. The innovative element in this approach is the applicability to high-dimensional climate models as is demonstrated by results obtained with the PLASIM climate model.

1 Introduction

In the year 2100, which is as far away (or as close) as 1932 in the past, mankind will be living on an Earth with, at least, a different climate than today. At that time, we will know the 2100-mean Global Mean Surface Temperature (GMST) value and its increase, say ΔT, above the pre-industrial GMST value. From the ~~GMST records of the 21^{nd} century~~then available GMST records, it will ~~then~~ also be known whether this change in GMST has been gradual or whether it was rather 'bumpy'. If the observational effort will continue as of today, there will ~~be also~~ also be an adequate observational record to determine whether the probability of extreme events (e.g., flooding, heat waves) has increased.

The outcomes of these future observations, to be made by our children and/or grandchildren, will strongly depend on socio-economic and technological developments and political decisions which are made now and over the next decades. Fortunately, there is a set of rational tools available to inform decision makers: Earth System Models. These models come in different flavours, from global climate models (GCMs) aimed to provide details on the development of the ocean-atmosphere-

ice-land system to integrated assessment models (AIMs) which also aim to describe the development of the broader socio-economic system. During the preparation for the fifth assessment report (AR5) of the Intergovernmental Panel of Climate Change (IPCC), GCM studies have focussed on the climate system response to GHG changes as derived by AIMs from different socio-economic scenario's scenarios; the data from these simulations is gathered in the so-called CMIP5 archive (Pachauri et al., 2014)(http://cmip-pcmdi.llnl.gov/cmip5/).

Depending on the representation of fast climate feedbacks in GCMs, determining their climate sensitivity, the CMIP5 models project a GMST increase ΔT of 2.5-4.5°C over the period 2000-2100 (Pachauri et al., 2014). This does not mean that the actual measured value of ΔT in 2100 will be in this interval. For example, the GMST may be well outside this range because of current model errors which misrepresented the strength of a specific feedback. As a consequence, a transition occurred in the real climate system during the period 2016-2100, which did not occur in any of the CMIP5 model simulations. Another possibility is that the GHG change development eventually was far outside of the scenario's scenarios considered in CMIP5.

A crucial issue in 2100 will be whether a climate state has been reached where a dangerous anthropogenic interference (DAI) can be identified (Mann, 2009). In this case, present-day islands will have been swallowed by the ocean, extreme events have increased in frequency and magnitude as envisioned in the Burning Embers diagram (Smith and Schneider, 2009). These effects are then very inhomogeneously distributed over the Earth and have lead to enormous socio-economic consequences. If this is the case in 2100, then there is a point in time where we must have crossed the conditions for DAI. This time, marking the boundary of a 'safe' and 'unsafe' climate state, obviously depends on the metrics used to quantify the state of the complex climate system.

In very simplified views, this boundary is interpreted as a threshold on pCO_2 (Hansen et al., 2008) or on GMST. The latter, in particular the $\Delta T_c = 2$°C threshold, has become an easy to communicate (and maybe therefore leading) idea to set mitigation targets for CO_2 greenhouse gas reduction. Emission scenario's scenarios have been calculated (Rogelj et al., 2011) such that ΔT will remain below ΔT_c. Although thresholds on GMST have been criticized for being very inadequate regarding impacts (Victor and Kennel, 2014), such a threshold (the aim is $\Delta T_c = 1.5$°C) forms the basis of policy making as is set forward in the Paris 2015 (COP21) agreement (the aim is $\Delta T_c = 1.5$°C).

Suppose that measures are being taken to keep $\Delta T < \Delta T_c$, does this mean that we are 'safe'? The answer is a simple no, as regionally still DAI may have occurred such as the disappearance of island chains due to sea level rise (Victor and Kennel, 2014). Hence, attempts have been made to define what 'safe' means in a more general way, such the Tolerable Windows Approach (TWA) (Petschel-Held et al., 1999) and Viability Theory (VT) (Aubin, 2009). These approaches also deal with general control strategies to steer a system towards '‘safety' when needed.

On a more abstract level, both TWA and VT start by defining a desirable (or 'safe') subspace V of a state vector $\mathbf{x}$ is in a general state space X. This subspace is characterized by constraints,

such as thresholds on properties of $\mathbf{x}$. ~~An exampleis the threshold $\Delta T < \Delta T_c$ on GMST, where~~ For example, when $\mathbf{x}$ is ~~in general~~ a high-dimensional state vector ~~in a GCM~~of a GCM, such a threshold could be $\Delta T < \Delta T_c$ on GMST. When the time-development (or trajectory) of $\mathbf{x}$ is such that it moves outside the subspace V, a control is sought to steer the trajectory back into V. Note that this is an abstract formulation of the mitigation problem, when the amplitude of the emission of greenhouse gases is taken as control. Recently, Heitzig et al. (2016) have added more detail to regions in the space X which differ in their 'safety' properties and amount of flexibility in control to steer to 'safety'.

Giving a certain desirable subspace of the climate system's state vector (~~i.e.~~e.g., to avoid DIA) and a suite of control options, (~~i.e.~~e.g., CO_2 emission reduction) it is important to know when it is too late to be able to steer the system to 'safe' conditions, say at the year 2100. In other words, when is the Point of No Return (PNR)? The TWA and VT approaches, and the theory in Heitzig et al. (2016), suffer from the ~~'~~'curse of dimensionality' and cannot be used within CMIP5 climate models. For example, the optimization problems in VT and TWA lead to dynamic programming ~~problems which have~~ schemes which have up to now only been solved for model systems with low-dimensional state vectors. The approach in Heitzig et al. (2016) requires the computation of region boundaries in state space, which also becomes tedious in more than two dimensions. Hence, with these approaches it will be impossible to determine a PNR using reasonably detailed models of the climate system.

In this paper, we present an approach similar to TWA and VT, but one which can be applied to high-dimensional models of the climate system. Key in the approach is the estimation of the probability density function of the properties of the state vector $\mathbf{x}$ which determine the 'safe' subspace V. The PNR problem is ~~also~~ coupled to limitations in the control options (e.g. of emissions) and can be defined precisely ~~within our approach~~using these options and stochastic viability theory. The more abstract formulation is presented in section 2~~below, building on stochastic viability theory and control strategies. Just~~ , and just to illustrate the concepts, we apply the approach in section 3 to an idealized energy balance model with and without ~~critical conditions (bifurcation behavior)~~tipping behavior. In section 4, the application to a high-dimensional climate model follows, using data ~~data~~ from the Planet Simulator (PLASIM, ~~(Fraedrich et al., 2005)). We combine these results with control strategies on GHG emissions and the associated cost functions (Stern, 2007) to find the PNR and optimal mitigation scenario for different GHG emission (RCP) scenario's using the PLASIM model.~~ Fraedrich et al. (2005)). A summary and discussion in section 5 concludes the paper.

2 Methodology

~~In this section~~ Here we briefly describe the concepts we need from stochastic viability theory and then define the PNR ~~specifically for~~ problem, specifically in the climate change ~~problem~~context.

2.1 Stochastic viability theory

Viability theory ~~basically~~ studies the control of the evolution of dynamical systems to stay within certain constraints on the system's state vector (Aubin, 2009). These constraints define a viable region V in state space. For a finite dimensional deterministic system, with state vector $\mathbf{x} \in R^d$ and vector field $\mathbf{f} : R^d \rightarrow R^d$, given by

$$\frac{d\mathbf{x}}{dt} = \mathbf{f}(\mathbf{x}, t), \tag{1}$$

an initial condition $\mathbf{x}_0 = \mathbf{x}(t = 0)$ is called viable if $\mathbf{x}(t) \in V$, for all $0 \leq t \leq t^*$, where t^* is a certain end time. The set of all these initial conditions forms the viability kernel associated with V. In a more general formulation of viability theory, an input is also considered in the right hand side of Eq. (1) which can be used to control the path of the trajectory $\mathbf{x}(t)$ in state space.

Stochastic extensions of viability theory consider finite dynamical systems defined by stochastic differential equations

$$d\mathbf{X_t} = \mathbf{f}(\mathbf{X}_t, t)dt + \mathbf{g}(\mathbf{X}_t, t)d\mathbf{W}_t, \tag{2}$$

where ~~$\mathbf{X}_t$~~ $\mathbf{X}_t \in R^d$ is a multidimensional stochastic process, ~~$\mathbf{W}_t$ the standard multidimensional Wiener process and the vector field $\mathbf{g}$~~ $\mathbf{W}_t \in R^n$ is a vector of n-independent standard Wiener processes and the matrix $\mathbf{g} \in R^{d \times n}$ describes the dependence of the noise on the state vector. The normalised probability density function (PDF) $p(\mathbf{x}, t)$ can be formally determined from the Fokker-Planck equation associated with Eq. (2).

A stochastic viability kernel V_β consists of initial conditions $\mathbf{X}_0$ for which the system has, for $0 \leq t \leq t^*$, a probability larger than a value β to stay in the viable region V (Doyen and De Lara, 2010). For example, in a one-dimensional version of Eq. (2) with state vector $X_t \in R$ and with a viable region V given by $x \leq x^*$ a state X_t is called viable, with tolerance probability β_T, if

$$\int_{-\infty}^{x^*} p(x, t)\, dx \geq \beta_T, \tag{3}$$

and otherwise, X_t is called non viable.

2.2 The Point of ~~no return~~No Return problem

In the climate change ~~problem, scenario's~~ context, scenarios of GHG increase and the associated radiative forcing have been formulated as Representative Concentration Pathways (RCPs). In Pachauri et al. (2014), there are four RCP scenarios (Fig. 1a) ranging from an increase in radiative forcing of ~~2.6 $\mathrm{Wm^{-2}}$~~ $2.6\,\mathrm{W\,m^{-2}}$ (RCP2.6) at 2100 (with respect to 2000) to ~~an increased forcing of 8.5 $\mathrm{Wm^{-2}}$~~ a forcing increase of $8.5\,\mathrm{W\,m^{-2}}$ (RCP8.5).

To define the PNR for each of these RCPs, a collection of mitigation ~~scenario's is~~ scenarios on greenhouse gas emission can be considered. These mitigation scenarios will lead to changes in GHG

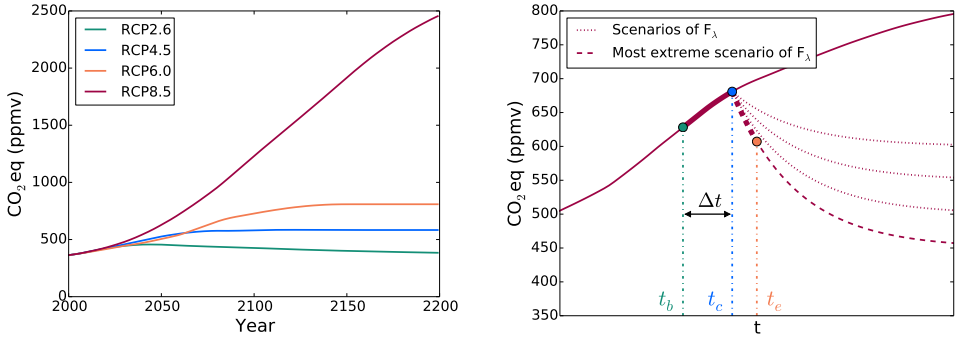

(a) (b)

Figure 1. *(a) CO_2eq trajectories of the RCP ~~scenario's~~ scenarios used by the IPCC in CMIP5. (b) The solid red curve represents a typical RCP scenario. At the time t_b the climate state becomes non-viable, while at $t = t_c$ a ~~mitigation scenario~~ CO_2eq reduction F_λ ~~is applied~~applies; at time t_e, the climate state is viable again.*

concentrations, described by functions $F_\lambda(t)$, where λ is a parameter. For instance, the collection F_λ could result from mitigation measures that lead to an exponential decay to different stabilisation levels (measured in CO_2 equivalent, or CO_2eq) within a certain time interval. An example of such a collection F_λ is shown by the dashed and dotted red lines in Fig. 1b. The most extreme member of F_λ is defined as the mitigation scenario (represented by a certain value of parameter λ) which has the steepest initial decrease at a certain time t (dashed curve in Fig. 1b).

~~When forcing a climate model with a~~ Along the curve of a certain RCP scenario, ~~its state vector $\mathbf{X}_t$ may not be viable anymore at a certain time . The first year of non viability of $\mathbf{X}_t$~~ there will be a point in time where action will be taken to reduce emissions of GHG; this is indicated by a time of action t_b. Consider for example (Fig. 1b) ~~. Once~~ that t_b is chosen as the first year where the state vector $\mathbf{X}_t$ is not viable ~~, ideally we want to control the~~ anymore. A reduction in emissions is, however, not immediately followed by a decrease in CO_2eq due to the long residence time of atmospheric CO_2~~eq concentration directly such that $\mathbf{X}_t$ will become viable again. However, reducing CO_2eq emissions is accompanied with~~ . In addition, there is a delay to take action in emission reduction due to technological, social, economic and institutional ~~challenge, and therefore mitigation will be delayed Δt years after the first year of non viability (Pachauri et al., 2014). The moment at which the~~ challenges. Hence, emission reduction will only start Δt_1 years after t_b. The CO_2eq ~~mitigation scenario is applied, is the time of action t_c; $t_c = t_b + \Delta t$. From the time of action,~~ will, even after emissions have been reduced, also still increase over a time Δt_2. The time at which the CO_2eq ~~concentration will decrease according to one of the mitigation scenarios in F_λ~~ starts to reduce according to F_λ is indicated by $t_c = t_b + \Delta t$, where $\Delta t = \Delta t_1 + \Delta t_2$. Eventually, $\mathbf{X}_t$ may become viable again and this point in time is indicated by t_e (Fig. 1b).

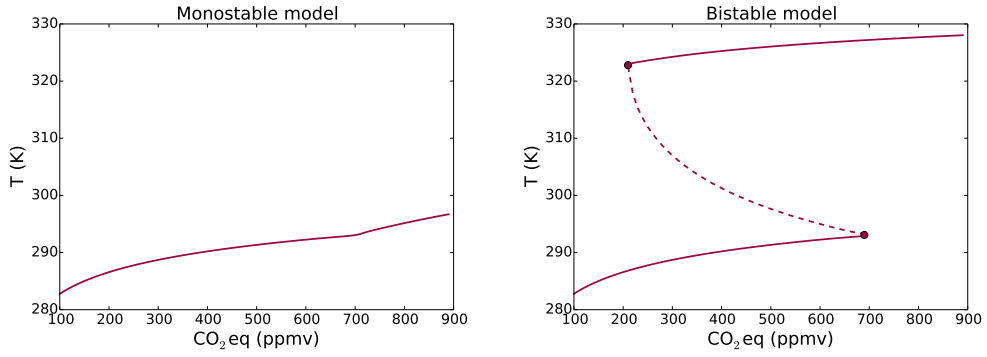

(a) (b)

Figure 2. *Bifurcation diagram of the deterministic energy balance model for $\alpha_1 = 0.45$ ((a), monostable model) and $\alpha_1 = 0.2$ ((b), bistable model). The solid ~~line~~ curve represents a stable equilibrium while a dashed ~~line~~ curve represents an unstable equilibrium.*

For a given RCP scenario, tolerance probability β_T, viable region V and collection F_λ, we define the PNR (π_t) as the first year t_c where, even when at that moment the most extreme ~~mitigation scenario of~~ CO_2eq reduction scenario F_λ ~~is applied~~applies,

(a) either $\mathbf{X}_t$ will be non viable for more than τ_T years, where τ_T is a set tolerance time, or

(b) $\mathbf{X}_t$ will be non viable in the year 2100.

The first PNR, which we will indicate below by π_t^{tol}, is based on limiting the amount of years that $\mathbf{X}_t$ is non viable, since (during these years) society is exposed to risks from, for example, extreme weather events. The second PNR, which we will indicate below by π_t^{2100} imposes no restrictions on how long $\mathbf{X}_t$ is non viable, but it only requires that $\mathbf{X}_t$ is non viable at the end on ~~the~~ this century. We will use both PNR concepts in the results below.

3 Energy balance model

In this section, we illustrate the concepts and the computation of the PNR for an idealized energy balance model of Budyko-Seller type (Budyko, 1969; Sellers, 1969). We will also assume that the CO_2eq can be directly controlled, and hence no carbon cycle model is needed to determine CO_2eq from an emission reduction scenario.

3.1 Formulation

We use the stochastic extension of the model formulation as in Hogg (2008). The equation for the atmospheric temperature T_t (in K) is given by

$$dT_t = \frac{1}{c_T}\left\{Q_0(1-\alpha(T_t)) + G + A\ln\frac{C(t)}{C_{ref}} - \sigma\epsilon {T_t}^4\right\}dt + \sigma_s dW_t. \tag{4}$$

The values and meaning of the parameters in Eq. (4) are given in Table 1. The first term in the right hand side of Eq. (4) represents the short-wave radiation received by the surface and $\alpha(T)$ is the albedo function, given by

$$\alpha(T) = \alpha_0 H(T_0 - T) + \alpha_1 H(T - T_1) + \big(\alpha_0 + (\alpha_1 - \alpha_0)\frac{T - T_0}{T_1 - T_0}\big) H(T - T_0) H(T_1 - T). \quad (5)$$

This equation contains the effect of land ice on the albedo and ~~$H(x) = (1 + \tanh(x/\epsilon_H))/2$~~ $H(x) = 1/2(1 + \tanh(x/\epsilon_H))$ is a continuous approximation of the Heaviside function. When the temperature $T < T_0$, the albedo will be α_0 and when $T > T_1$ it will be α_1 and the albedo is linear in T for $T \in [T_0, T_1]$. The second term in the right hand side of Eq. (4) represents the effect of greenhouse gases on the temperature. It consists of a constant part (G), and a part ($A \ln \frac{C(t)}{C_0}$) depending on the mean CO_2eq concentration in the atmosphere (indicated by $C(t)$). The third term in the right hand side of Eq. (4) expresses the effect of long-wave radiation on the temperature and the last term represents noise with a constant standard deviation σ_s. The standard value of σ_s ~~is such that the variance of the noise (σ_s^2) is~~ chosen as 3% of the value of G/c_T, hence about $0.3K$/year. The variance in CO_2 concentration originates mostly from seasonal variations, ~~but~~ and the 3% is on the high side. Nevertheless, we still use this value, because if we take values smaller than 3% the PDF of the GMST will almost be a delta function and concepts can not be illustrated clearly.

3.2 Results: stochastic viability kernels

When using the global mean CO_2eq concentration C in Eq. (4) as a time-independent control parameter, a bifurcation diagram can be easily (numerically) calculated for the deterministic case ($\sigma_s = 0$). In Fig. 2, such diagrams are plotted of C versus the equilibrium temperature T for two values of α_1. To obtain realistic values for the temperature, the equilibrium temperature equilibria are shifted upwards by 30 K. This is done by substituting T with $T - 30$ and adapting the right hand side of Eq. (4) such that the new temperature is a steady state. This is obviously a bit artificial here, but we justify it by our aim to only wanting to illustrate the methodology; results from more realistic models will follow in section 4 below. The diagram corresponding to $\alpha_1 = 0.2$ (Fig. 2a) has two saddle-node bifurcations which are absent for $\alpha_1 = 0.45$ (Fig. 2b). From now on, the energy balance model with $\alpha_1 = 0.45$ and $\alpha_1 = 0.2$ will be called ~~monostable case~~ the monostable and bistable case, respectively.

For $\sigma_s \neq 0$, we explicitly determine the normalised PDF $p(x,t)$. Rewriting Eq. (4) as

$$dT_t = f(T_t, t)dt + \sigma_s dW_t, \quad (6)$$

with $f(T,t) = c_T^{-1}(Q_0(1 - \alpha(T)) + G + A \ln \frac{C(t)}{C_{ref}} - \sigma\epsilon T^4)$, the Fokker-Planck equation of Eq. (6) is given by

$$\frac{\partial p}{\partial t} + \frac{\partial (fp)}{\partial x} - \frac{\sigma_s^2}{2}\frac{\partial^2 p}{\partial x^2} = 0. \quad (7)$$

Table 1. *Value and meaning of the parameters in the energy balance model given by Eq. (4).*

c_T	5.0×10^8 Jm^{-2}K^{-1}	Thermal inertia	ϵ	1.0	Emissivity
Q_0	342 Wm^{-2}	Solar constant/4	α_0	0.7	Albedo parameter
G	1.5×10^2 Wm^{-2}	Constant	α_1	0.2 or 0.45	Albedo parameter
A	2.05×10^1 Wm^{-2}	Constant	T_0	263 K	Albedo parameter
C_{ref}	280 ppmv	Reference CO_2 concentration	T_1	293 K	Albedo parameter
σ	5.67 x 10^{-8} Wm^{-2}K^{-4}	Stefan Boltzmann constant	ϵ_H	0.273 K	Albedo parameter

This differential equation is solved numerically for $p(x,t)$ under any prescribed function $C(t)$ with boundary conditions $p(x_u,t) = p(x_l,t) = 0$, where x_l = 270 K and x_u = 335 K, and an initial condition $p(x,0)$ (specified below) satisfying $\int_{x_l}^{x_u} p(x,0)dx = 1$.

We first show stochastic viability kernels for each initial condition T_0 and C_0, where C_0 is an initial CO_2eq concentration and T_0 is the expectation value of the initial PDF of T_t. As starting time, we take the year 2030 and suppose that the climate system will be forced by a certain RCP scenario from 2030 till 2200. For every C_0, the original RCP scenario from Fig. 1a is adjusted such that its time development remains the same, but it has C_0 as CO_2eq concentration in 2030. The PDF of the GMST $p(x,t=0)$ ($t=0$ refers to the year 2030) has a prescribed variance (defined by σ_s^2) and an expectation value T_0.

In Fig. 3, the stochastic viability kernels are plotted for the energy balance model forced by the RCP4.5 scenario and a viable region V defined by $T \leq 293$ K. The results for the monostable and bistable cases are plotted in Fig. 3a and Fig. 3b, respectively. The colors indicate for each combination of T_0 and C_0 in which stochastic viability kernel the initial state (C_0, T_0) is located. For example, consider the bistable case and an initial condition of $T_0 = 288$ K and $C_0 = 400$ ppmv, then this initial condition is in the kernel V_β with $\beta \geq 0.9$. This means that, with a probability larger than 0.9, a trajectory of the model starting at (C_0, T_0) will remain viable up to the year 2200, where C follows the RCP4.5 scenario. The white areas contain initial conditions that are in a stochastic viability kernel V_β with $\beta < 0.5$.

The sensitivity of the stochastic viability kernels with respect to RCP scenario, threshold defining the viable region V and amplitude of the noise σ_s was also investigated (results not shown). The behaviour is as one can expect in that the area of the kernels becomes smaller (larger) when noise is larger (smaller), when the threshold temperature is smaller (larger) and when the radiative forcing associated with the RCP scenario is more (less) severe. For example for the RCP6.0 scenario, each combination of T_0 and C_0 (same range as in Fig. 3) is in a V_β with $\beta < 0.5$ for both mono- and bistable cases.

3.3 Results: Point of No Return

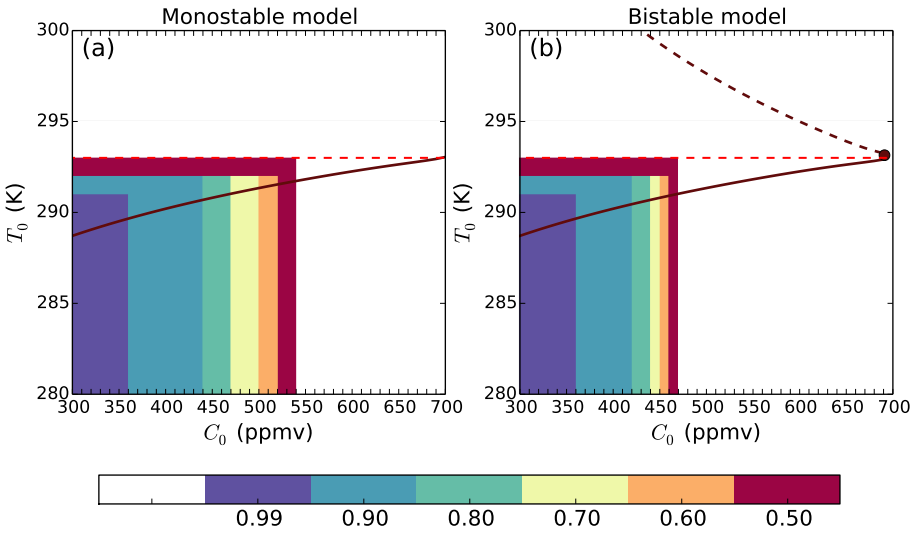

Figure 3. The stochastic viability kernels for the monostable and bistable cases forced by the RCP4.5 scenario. The viable region is defined as $T \leq 293K$ and is indicated by the red dashed line. This plots show, for each combination of T_0 and C_0, in which stochastic viability kernel these initial values are located. The numbers in the colourbar stand for the β in V_β. For convenience, the bifurcation diagram of the deterministic model is also shown.

Again for illustration purposes, we assume that reduction of the emissions will have an immediate effect of the CO_2eq, such that effectively the CO_2eq is controlled. We choose the collection F_λ to consist of mitigation scenarios that exponentially decay to the preindustrial CO_2eq concentration, which is 280 ppmv. For this exponential decay, we consider different e-folding times ~~, which is indicated by the parameter~~ τ_d. ~~As most extreme mitigation scenario~~ The most extreme scenario has an exponential decay within 50 years~~is considered~~, which corresponds to an e-folding time of $\tau_d = 9$ years. ~~Finally~~Hence, the collection F_λ ~~consist of mitigation scenarios for which~~ is given by (for $\tau_d \geq 9$~~years. A mitigation scenario with an e-folding time of τ_d years is then given by~~)

$$F_\lambda(t) = (C_{t_c} - 280)\exp\left(-\frac{t - t_c}{\tau_d}\right) + 280. \tag{8}$$

In this equation, t_c is the time at which the ~~mitigation~~ scenario is applied and C_{t_c} the associated CO_2eq concentration at that moment.

Next, we determine PNR values π_t^{tol} for the energy balance model when it is forced by the four different RCP scenarios using a tolerance probability of $\beta_T = 0.9$ and a tolerance time of $\tau_T = 20$ years. The π_t^{tol} values for a system forced with the RCP4.5, RCP6.0 and RCP8.5 ~~scenario's~~ scenarios are shown in Fig. 4 for both the monostable and bistable cases. As expected, the more extreme the RCP scenario, the earlier the PNR. This can be easily explained by the fact that when the CO_2eq concentration is rising faster, the temperature will get non viable earlier. Consequently, the PNR will be earlier, since the GMST is only allowed to be non viable for at most τ_T years. When the

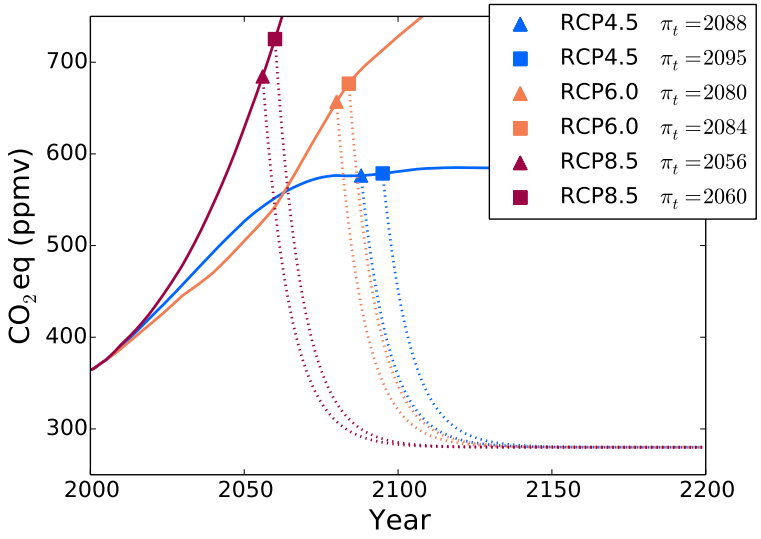

(a)

Figure 4. The PNR π_t^{tol} for a system forced with different RCP scenarios, tolerance probability $\beta_T = 0.9$ and tolerance time ~~$\tau_T = 20$~~ $\tau_T = t_e - t_b = 20$ years and $\Delta t = 0$. The triangles indicate the point of no return for the bistable case and the squares for the monostable case. The dotted line is the most extreme scenario of F_λ with an exponential decay to 280 ppmv and an e-folding time of 9 years. Note that for both cases there is no PNR when the model is forced with the RCP2.6 scenario.

model is forced with RCP2.6, there is no PNR for both models. The reason for this is that the CO_2eq concentration will remain low throughout the whole period and consequently the temperature will stay viable. The value of π_t^{tol} of the bistable case is for each scenario earlier than the value of the monostable case. This can be clarified by the fact that the PDF of the temperature in the bistable case will leave the viable region at a lower CO_2eq concentration because of the existence of nearby equilibria.

The sensitivity of π_t^{tol} versus the tolerance time τ_T and the tolerance probability β_T was also investigated and the results are as expected (and therefore not shown). A longer tolerance time will shift π_t^{tol} to later times. For example, for the RCP4.5 scenario $\pi_t^{tol} = 2071,\ 2088$ and 2116 for $\tau_T = 0, 20$ and 50 years for the bistable case (for fixed $\beta_T = 0.9$). With a fixed $\tau_T = 20$ years, the value of π_t^{tol} shifts to smaller values when the tolerance probability is increased. For example, for $\beta_T = 0.80$ and 0.99, the values of π_t^{tol} are 2127 and 2058, respectively, for the bistable case (for $\beta_T = 0.9$, ~~it is 2088~~ $\pi_t^{tol} = 2088$, see Fig. 4).

4 PLASIM

The results in the previous section have illustrated that a PNR can be calculated when an estimate of the probability density function can be calculated and a collection of mitigation ~~scenario's~~ scenarios

is available. We will now apply these concepts to the more detailed, high-dimensional, climate model PLASIM, a General Circulation Model developed by the University of Hamburg~~, and using mitigation scenario's derived from those suggested in the IPCC - AR5 report.~~. A main problem here is to determine a relation between the CO_2eq (and associated radiative forcing) and the GMST, i.e. a response function. Previous approaches have used a fit of a specific response function (e.g., a power law function) to available observations (Rypdal, 2016). This is more complicated for an approach using stochastic viability theory and hence we proceed along another path.

4.1 Linear response theory

In order to find the temporal evolution of the PDF of the global mean surface temperature GMST (indicated by T) under any CO_2eq forcing in PLASIM, we will use linear response theory (LRT). With this theory, the effect of any small forcing perturbation on the system state can be calculated by running the climate model for only one forcing scenario (Ragone et al., 2014).

In LRT, the expectation value of an observable Φ, when forcing the system with a time-dependent function $f(t)$, can be calculated by computing the convolution of a Green's function $G_{\langle\Phi\rangle}$ and the forcing $f(t)$, according to

$$\langle\Phi\rangle_f(t) = \int_{-\infty}^{+\infty} G_{\langle\Phi\rangle}(\tau) f(t-\tau) d\tau. \tag{9}$$

To construct this Green's function, the property that the convolution in the time domain is the same as point-wise multiplication in the frequency domain is used. The Fourier transform of Eq. (9) is given by

$$\langle\widetilde{\Phi}\rangle_f(\omega) = \chi_{\langle\Phi\rangle}(\omega)\widetilde{f}(\omega), \tag{10}$$

with $\chi_{\langle\Phi\rangle}(\omega)$, $\langle\widetilde{\Phi}\rangle_f(\omega)$ and $\widetilde{f}(\omega)$ being the Fourier transforms of $G_{\langle\Phi\rangle}(t)$, $\langle\Phi\rangle_f(t)$ and $f(t)$, respectively. Therefore, once the time evolution of the expectation value of an observable under a certain forcing is known, the Green's function of this observable can be constructed with Eq. (10) and consequently the linear response of the observable to any forcing can be calculated.

We use the same data as in Ragone et al. (2014), provided by F. Lunkeit and V. Lucarini (Univ. Hamburg, Germany). The difference with those in Ragone et al. (2014) is that the seasonal ~~cycle is not removed. This~~ forcing is present, which results in a long-term increase of the GMST of 5 °C (instead of 8 °C in Ragone et al. (2014)) under a scenario where the CO_2 concentration doubles. The reason of this difference is not fully clear but probably result from seasonal rectification effects of nonlinear feedbacks. Data of GMST from two ensembles was used, each of 200 simulations, made with two different CO_2 forcing profiles (all other GHGs are kept constant). For both forcing profiles, the starting CO_2 concentration is set to a value of 360 ppmv, which is representative for the CO_2 concentration in 2000. During the first set of experiments, the CO_2 concentration is instantaneously

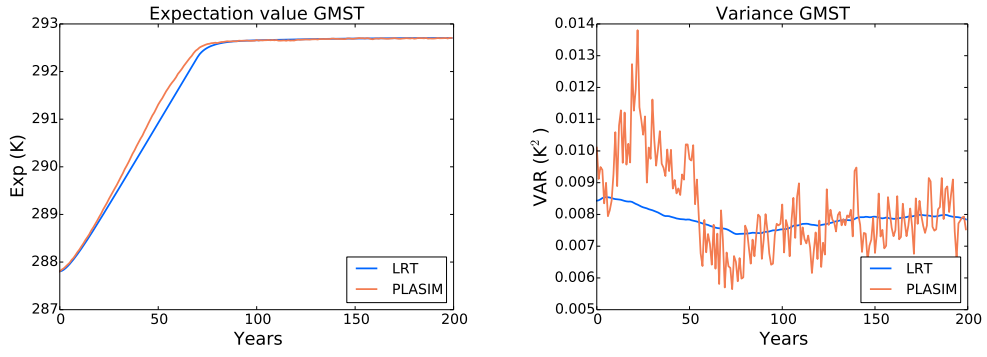

(a) (b)

Figure 5. *(a) The expectation value and (b) variance of GMST generated by PLASIM (orange) and determined through LRT (blue) for the 1% CO_2 concentration increase.*

doubled to 720 ppmv and kept constant afterwards. During the second set of experiments, the CO_2 concentration increases each year ~~with~~ by 1 % until a concentration of 720 ppmv is reached. This will take approximately 70 years and afterwards the concentration is fixed. The total length of the simulations is 200 years. Furthermore, the forcing $f(t)$ in Eq. (9) is the logarithm of the CO_2 concentration, since the radiative forcing scales approximately logarithmically with the CO_2 concentration.

~~In order to~~ To determine the PDF of GMST under any CO_2eq forcing, we make the assumption that at each point in time the PDF of the GMST is normally distributed. As we have 200 data points for the GMST at each time interval, a χ^2 test was used to analyse the PDFs. For each time, the value of $\chi^2 > 0.05$ and therefore the assumption that the PDF of the GMST is normally distributed appears justified. The Green's functions for the expectation value and variance of GMST have been calculated with the instantaneously doubling CO_2 profile and the associated ensemble. From the ensemble, at each point in time the expectation value and variance are calculated such that we get the temporal evolution of these two variables. Subsequently, we have found the Green's functions ~~with~~ using (10). To check whether these Green's functions perform well, we ~~compare~~ compared the temporal evolution of the expectation value and variance of the GMST under the 1 % forcing (calculated with (9)) with those directly generated with PLASIM (Fig. 5). The expectation value ~~made~~ determined with LRT is close to the one directly generated by PLASIM. However, the variance of the ensemble generated by PLASIM is a lot noisier than the one ~~made~~ calculated with LRT. Although the Green's function of the variance provides only a rough approximation, it has the right order of magnitude and we will use it to calculate the variance of the GMST for other forcing ~~scenario's~~scenarios.

4.2 Results: Point of No Return under CO_2eq control

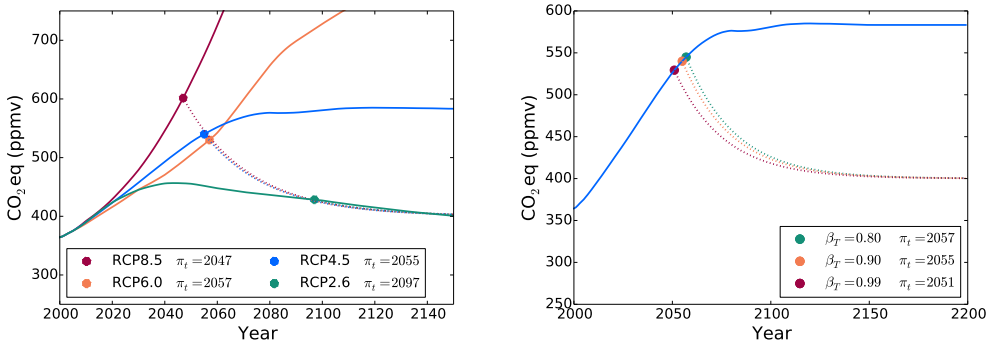

(a) (b)

Figure 6. *(a) The PNR π_t^{2100} for the RCP2.6, RCP4.5, RCP6.0 and RCP8.5 scenarios for a tolerance probability of $\beta_T = 0.9$ and $\Delta t = 0$. The solid lines represent the RCP scenarios and the dashed line the most extreme scenario from F_λ. Note that these dashed lines coincide. (b) The point of no return for RCP4.5 for different tolerance probabilities.*

~~The mitigation scenarios in~~ We first consider the case without a carbon cycle model, again assuming that the CO_2eq concentration can be controlled directly. The scenarios F_λ ~~considered~~ chosen for use in PLASIM are exponentially decaying to different stabilisation levels (varying between 400 and 550 ppmv, see Edenhofer et al. (2010)). This stabilization level is taken as the parameter λ. We assume that stabilisation happens within 100 years, which corresponds to an e-folding time τ_d of about 25 years; the mitigation scenarios F_λ are then given by

$$F_\lambda(t) = \big(C_{t_c} - \lambda\big) \exp\Big(-\frac{t - t_c}{\tau_d}\Big) + \lambda, \tag{11}$$

where t_c is again the time at which the mitigation scenario is applied and C_{t_c} the associated CO_2eq concentration. The most extreme mitigation scenario in F_λ in terms of CO_2eq decrease is the one that stabilises at a CO_2eq concentration of 400 ppmv.

We next determine the PNR π_t^{2100} by requiring that the GMST must be viable in 2100 using a tolerance probability of $\beta_T = 0.90$. Furthermore, the viable region is set at $T \leq 16.15°$C, which corresponds to temperatures ~~lower~~ less than 2°C above the preindustrial GMST. The values of π_t^{2100} for all the RCP scenarios are plotted in Fig. 6a. ~~The solid lines represent~~ Solid curves show the RCP scenarios ~~and the dashed lines~~ while dashed curves present the most extreme scenario ~~from~~ F_λ. ~~The value of π_t^{2100} for the~~ For RCP8.5~~forcing~~, π_t^{2100} is 10 years ~~smaller than that for the~~ earlier than for RCP6.0~~scenario~~, since the CO_2eq concentration increases much faster for the RCP8.5 scenario. ~~However, the~~ The mitigation scenario after the point of no return, represented by the dashed line, is the same for all RCP scenarios~~the same~~. This is related to ~~the~~ our definition of π_t^{2100}, where it is required that the GMST is viable in 2100. The mitigation scenario that is plotted is the ultimate scenario that guarantees this. It indicates that ~~(if the mitigation scenario plotted in Fig. 6a is extended for years smaller than 2047) for~~ for each CO_2 scenario the associated π_t^{2100} is given by the intersection

of that CO_2eq scenario and the mitigation scenario. This is because it is considered that an exponential decay to 400 ppmv within 100 years is always possible, no matter the CO_2eq concentration at t_c. However, when this concentration becomes too high, this mitigation scenario is not ~~realistic anymore (as discussed in the next subsection)~~very realistic anymore.

The influence of the tolerance probability on π_t^{2100} for the RCP4.5 scenario is plotted in Fig. 6b, where we only consider a tolerance probability of 0.8, 0.9 and 0.99. When the tolerance probability is higher, it takes longer before the GMST will be viable again and thus the PNR π_t^{2100} will be earlier. However, the differences are very small, since the mitigation scenarios that guarantee viability in 2100 for the different tolerance probabilities are very close~~to each other~~.

4.3 Results: ~~Optimal mitigation scenario~~Point of No Return under emission control

~~(a) (b) (a) The expected rise of GDP expressed in US dollars and (b) the annual economic costs of stabilising after 100 years at CO_2eq levels of 400 ppmv and 550 ppmv. Both figures are from Edenhofer et al. (2010) and show results of the POLES model. Note that to calculate the annual costs of stabilising at another CO_2eq level, for each year we linearly interpolate the costs. The approach followed here also provides the possibility to determine an optimal mitigation strategy as each of these mitigation scenario's has its own economic costs. The costs associated with the stringency of mitigation are determined using the output of the POLES model. This is an energy-environment-economy model and used by Edenhofer et al. (2010) to calculate the economics of low~~ Finally, we consider the more realistic case where emissions are controlled and a carbon model converts emissions to CO_2eq~~stabilisation. Fig. ??(a) reveals how the POLES model expects the global gross domestic product (GDP, below indicated by $\mathcal{G}$) to increase till 2100. The annual costs of stabilising at~~ . A simple carbon model relating emissions E to concentrations C is given by

$$C_{CO2}(t) = C_{CO2,0} + \int_0^t G_{CO2}(\tau)\, E_{CO2}(t-\tau)\, d\tau, \tag{12}$$

where $C_{CO2,0}$ is the initial concentration. The Green's function for CO_2 ~~eq levels of 400 ppmv and 550 ppmv~~ is taken directly from Joos et al. (2013):

$$G_{CO2}(t) = a_0 + \sum_{i=1}^{3} a_i e^{t/\tau_i}, \tag{13}$$

where the parameters are shown in ~~Fig. ??(b) (Edenhofer et al., 2010); the costs are expressed in percentage of the GDP. The cost for stabilising at 400 ppmv are a lot higher than for stabilising at 500 ppmv. This is because such a low stabilisation can only be reached when new technologies, like energy made out of biomass and carbon storage, are used on a large scale~~Table 2. The quantity E_{CO2} is the CO_2 emission in $\mathrm{ppm\,yr^{-1}}$ that has been converted from $\mathrm{GtC\,yr^{-1}}$ using the Carbon molecular weight as $E_{CO2}[\mathrm{ppm\,yr^{-1}}] = \gamma\, E_{CO2}[\mathrm{GtC/yr}]$, with $\gamma = 0.46969\,\mathrm{ppm\,GtC^{-1}}$. The

emissions for the RCP scenarios are taken from Meinshausen et al. (2011) [1]. The carbon model underestimates CO_2 levels for very high emission scenarios as it does not include saturation of natural CO_2 sinks.

~~In order to calculate the economic costs of a mitigation scenario that stabilises at a certain~~ Following Table 8.SM.1 of Myhre et al. (2013) we obtain the changes in radiative forcing compared to preindustrial (in $\mathrm{W\,m^{-2}}$) due to changes in CO_2 ~~eq level, the following assumptions are made.~~ as ~~The annual costs of a mitigation scenario that stabilises at another~~

$$\Delta F_{CO2} = \alpha_{CO2} \ln \frac{C_{CO2}}{C_0}, \tag{14}$$

where C_0 is the pre-industrial (1750) CO_2 ~~eq level than 400 or 550 ppmv are linearly interpolated from the costs at these two values. Costs are only dependent on the stabilization level and are independent of the~~ concentration.

We use the same PLASIM ensemble of instantaneous CO_2 ~~eq concentration at t_c ($C(t_c)$) . To determine the dependence on $C(t_c)$ would require an analysis of different mitigation scenarios than in Edenhofer et al. (2010) and this is beyond the scope of this study. Costs are taken into account only for mitigation between $t = t_c$~~ doubling runs again to determine a Green's function that relates radiative forcing changes to temperature changes as

$$\Delta T(t) = \int_0^t G_T(\tau) \Delta F(t-\tau) d\tau \tag{15}$$

where G_T is the data-based function determined from LRT. The total radiative forcing is taken as $\Delta F_{tot} = A \Delta F_{CO2}$, where we introduce a scaling constant A to correct for the high climate sensitivity of the PLASIM model compared to typical CMIP5 models. Based on trial runs attempting to reconstruct mean CMIP5 RCP temperature trajectories with RCP CO_2 emissions we choose $A = 0.6$.

For PLASIM, the Green's function G_T, as determined through LRT, is well approximated by a one-time scale exponential:

$$G_T(t) \approx b_1 e^{-t/\tau_{b1}}, \tag{16}$$

with $b_1 = 0.25\,\mathrm{K\,W^{-1}\,m^2\,yr^{-1}}$ and ~~$t = 2100$~~ $\tau_{b1} = 4.69\,\mathrm{yr}$. ~~The annual GDP loss associated with a scenario that stabilises at $\lambda = C_{st}$ is indicated by the function $\mathcal{G}^{\lambda}_{mit}(t)$.~~

~~When the temperature reaches a value of 2°C above the preindustrial temperature, Stern (2007) estimated the annual costs associated with damage of extreme weather events at 0.5-1.0% of the GDP. We have chosen here to charge 1.0% GDP ($\mathcal{G}_{ewe}$ below) for every year the GMST is not viable; when the temperature is viable, no costs will be charged. Consequently, the~~

[1] See the database at http://www.pik-potsdam.de/~mmalte/rcps/

costs associated with the stringency of mitigation for a mitigation scenario are given by

$$\Psi\big(F_\lambda(t)\big) = \frac{1}{100}\Big(\sum_{t=t_c}^{2100} \mathcal{G}(t)\, \mathcal{G}^{\lambda}_{mit}(t) + \sum_{t=t_b}^{t_e} \mathcal{G}(t)\, \mathcal{G}_{ewe}\Big)$$

We determine a Green's function for the temperature variance in the same way.

The optimal mitigation scenario can be found by minimising the cost function Ψ under the restriction that the climate must be viable in 2100. As an example, we consider the forcing according to the

Table 2. Model Parameters. No units are given for dimensionless parameters

$C_{CO2,0}$ (ppm)	278	α_{CO2}	5.35	C_0 (ppm)	278
a_0	0.2173	A	0.6	γ (ppm GtC^{-1}	0.46969
a_1	0.2240	a_2	0.2824	a_3	0.2763
τ_1 (yr)	394.4	τ_2 (yr)	36.54	τ_3 (yr)	4.304

To compute the Point of No Return π_t^{2100} in the carbon-climate model we start from pre-industrial CO_2 concentrations and take the corresponding initial temperature perturbation as $\Delta T = 0$. We then prescribe the RCP emissions scenarios for RCP2.6, RCP4.5scenario, where the first year of non viability is 2027. For $\Delta t = 4$ years, , RCP6 and RCP8.5 (that are identical up to the year 2005). At a year $t_b > 2005$ we start reduction of emissions at an exponential rate, i.e. for $t > t_b$ the emissions follow

$$E_{CO2}(t) = E_{CO2}(t_b) \exp\left(-\frac{t - t_b}{\tau_e}\right) \tag{17}$$

where $\tau_e = 25\,\mathrm{yr}$ is the year when mitigating is started is 2031. In Fig. **??**a, the costs are plotted for the different mitigation scenarios. Stabilisation concentrations of 425 ppmv and higher are not considered, since these scenarios do not guarantee that the GMST is viable in 2100. The optimal mitigation scenario is a scenario that stabilises at a COe-folding timescale of the emission reduction that we keep constant. Using the carbon model we compute the instantaneous CO_2 concentrations for each such scenario and use the Green's functions for GMST mean and variance to determine the PDF at year 2100 for each starting year t_b. Assuming Gaussian distributions (this is well satisfied for the original PLASIM ensemble), we can then easily determine the temperature threshold below which 90% of the values fall. The first year for which this threshold is above 2 K gives π_t^{2100}. Note that the value of t_c (in Fig. 2b) where the CO_2 eq concentration of 412.4 ppmv. starts to decrease is determined by the coupled carbon-climate model.

The warming in 2100 predicted by our simple climate model when starting exponential CO_2 emission reduction in a given year is shown in Fig. 7a. The intersections between the RCP curves

~~(a)~~ ~~(b)~~

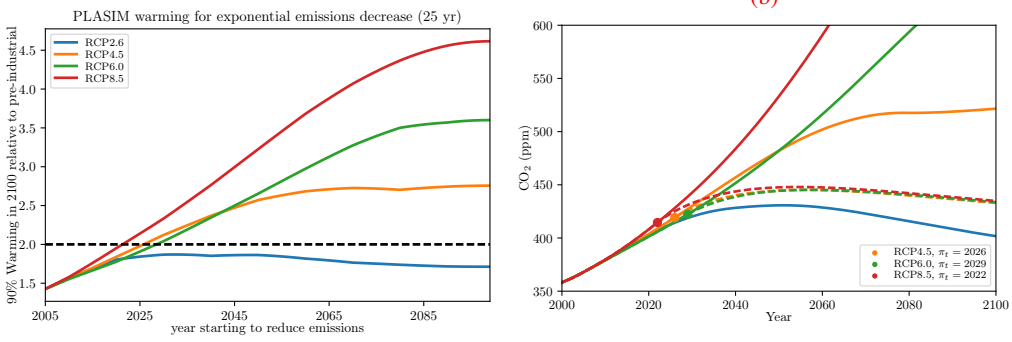

(a) (b)

~~The costs for the different mitigation scenarios for the case of RCP4.5, $\beta_T = 0.9$ and $\Delta t = 4$ years. On the horizontal axis is the stabilisation CO_2eq level of the scenarios in F_λ. The optimal mitigation scenario is shown by the orange dot. The associated costs can be found in the legend. (b) The costs of the optimal mitigation scenario for different Δt. The point of no return π_t^{2100} corresponds to $\Delta t = 28$ years.~~

Figure 7. *(a) Warming in 2100 when starting exponential CO_2 emission reduction in a given year. (b) CO_2 concentration for the four RCP scenarios as computed by the model (solid) and following exponential mitigation starting from the Point of no Return (dashed).*

(solid color) and the dashed line (giving 2 K warming) provide values of π_t^{2100}. Values do not differ much for the different RCP (4.5, 6.0 and 8.5) scenarios and are before 2030. RCP2.6 does not have a Point of No Return as its emission scenario is sufficient to keep the warming safely below 2 K. The counter-intuitive lowering of the curve for RCP2.6 (also slightly for RCP4.5) is due to very fast emission reductions in these RCP scenarios. So starting emission reduction at later times may lead to lower total emissions (and hence, temperatures). The CO_2 concentration for the four RCP scenarios as computed by the model (solid) and following the exponential mitigation starting from the Point of no Return (dashed) are shown in Fig. 7b. Note how emissions 'still in the pipeline' lead to CO_2 increases even after the reduction is initiated. ~~The wiggles in Fig. **??**a can be explained by the fact that for some scenarios the amount of years of non viability are the same. However,~~ Note that this approach does not factor in the uncertainty in the carbon model as we do not have a Green's function propagating the carbon uncertainty through the temperature model. Including this would very likely increase the variance in the pdf and move the Point of No Return to an earlier year. On the other hand, the ~~period of the wiggles gets smaller as the stabilisation CO_2eq concentration increases. To explain this , we note that the moment of getting viable again (t_e) corresponds with a certain reference CO_2eq concentration. During low stabilisation, the decrease in CO_2eq concentration is steep and there is not much time between the intersection of two consecutive mitigation scenarios with this reference concentration. However, when the stabilisation concentration is higher, the decrease in CO_2eq concentration will be less steep, and there is more time between the intersection of two consecutive scenarios and the reference concentration.~~

~~Fig~~PLASIM variance is quite small, so the 90% threshold is not vastly different from the mean. ~~??bshows how the costs of the optimal mitigation scenario change when Δt increases . The results in Fig. ??a are for $\Delta t = 4$ years and $\Delta t = 28$ years corresponds with the point of no return. Fig. ??breveals that there is a Δt that maximises the costs of the optimal mitigation scenario. When Δt increases, the time between t_b and t_c will increase and thus the costs associated with extreme weather events increases. Also, when Δt increases, the optimal mitigation scenario is steeper and thus more expensive. However, since the time between t_c and 2100 will decrease as well, the total costs associated with the stringency of mitigation eventually decrease for larger values of Δt.~~

5 Discussion

Pachauri et al. (2014) stated with high confidence that: "Without additional mitigation efforts beyond those in place today, and even with adaptation, warming by the end of the 21st century will lead to high to very high risk of severe, widespread and irreversible impacts globally". If no measures are taken to reduce GHG emissions during this century and neither will there be any new technological developments that can reduce GHGs in the atmosphere, it is likely that the GMST will be 4 °C higher than the preindustrial GMST at the end of the 21st century (Pachauri et al., 2014). Consequently, it is important that anthropogenic emissions are regulated and significantly reduced before widespread and irreversible impacts occur. It would help motivate mitigation when we would know when it is ~~"too late"~~'too late'.

In this study we have defined the concept of the Point of No Return (PNR) in climate change more precisely, using stochastic viability theory and a collection of mitigation ~~scenario's~~scenarios. For an energy balance model, as in section 3, the probability density function could be explicitly computed and hence stochastic viability kernels ~~were determined. In this model , the PNR was~~ could be determined. The additional advantage of this model is that one can easily construct a bistable regime, so one can investigate the effects of tipping behavior on the PNR. We used this model (where the assumption was made that CO_2 could be controlled directly instead of through emissions), to illustrate of concept of PNR which is based on a tolerance time for which the climate state is non viable. For the RCP ~~scenario's~~ scenarios considered, one finds that the PNR is smaller in the bistable than in the monostable regime of this model. The occurrence of possible transitions to warm states in this model indeed cause ~~it~~ the PNR to be 'too late' earlier.

~~Key~~ The determination of the PNR in the relatively high-dimensional PLASIM climate model, however, shows the key innovation in our approach, ~~however, is to use~~ i.e. the use of linear response theory (LRT) ~~for high-dimensional models~~ to estimate the probability density function. ~~We showed this by computing PNRs for the PLASIM model (section 4), where the PNR is~~ PLASIM was used to compute another variant of a PNR based on only requiring that the climate state is viable in the year 2100. In the PLASIM results, we used a viability region that was defined as GMSTs lower than

2°C above the pre-industrial value~~. This 2°C level gained a lot of prominence in the early 1990s when a number of international scientific panels suggested that it would prevent some of the worst impacts of climate change. Recently, during the 2015 Paris Climate Conference (COP21), it was decided that 1.5°C is a significantly safer threshold. With~~ , but with our methodology, the PNR can be easily determined for any threshold defining the viable region. The more academic case where we assume that GHG levels can be controlled directly provides PNR (for RCP4.5, RCP6.0 and RCP8.5) values around 2050 (section 4.2). However, the more realistic case where the emissions are controlled (section 4.3) and a carbon model is used, reduces the PNR for these three RCP scenarios by about 30 years. The reason is that there is a delay between the decrease in GHG gas emissions and concentrations.

Although our approach provides new insights into the ~~point of no return~~ Point of No Return in climate change, we recognize there is potential to substantial further improvement. ~~The assumption about the most extreme scenario from F_λ, here considered to be an exponential decay to 400 ppmv within 100 years, is too simplified. Once, the CO_2eq concentration at t_c is very high, this is an unrealistic scenario. Therefore, further research must be done to determine the most extreme mitigation scenario for each CO_2eq concentration. We also designed a rather idealized cost function to find the optimal mitigation scenario in PLASIM . The costs associated with the stringency of the mitigation scenario are calculated using the POLES model. In this model the economic costs are given for one specific CO_2eq scenario that stabilises at 400 ppmv. However, we use these costs to calculate the costs for any scenario that stabilises at 400 ppmv, no matter the CO_2eq concentration at t_c~~First of all, the PLASIM model has a too high climate sensitivity compared to CMIP5 models. Although in the most realistic case (section 4.3), we somehow compensate for this effect, it would be much better to apply the LRT approach to CMIP5 simulations. However, a large ensemble such as that available for PLASIM is not available (yet) for any CMIP5 model. Second, in the LRT approach, we assume the GMST distributions to be Gaussian. This is ~~a shortcoming in our cost function which can be improved by using the POLES model to calculate the costs for each separate mitigation scenario.~~ well justified in PLASIM, as can be verified from the PLASIM simulations, but it might not be the case for a typical CMIP5 model. Third, for the more realistic case in section 4.3, we do not capture the uncertainties in the carbon model and hence in the radiative forcing.

~~Another shortcoming in the cost function lies in the part that calculates the costs associated with extreme weather events. We only charge costs for extreme weather events when the GMST is not viable. Also, for each year that the GMST is not viable, no matter the height of the GMST, the costs are given by the same percentage of the GDP. Furthermore, we only consider costs associated with stringency of mitigation and extreme weather events. However, there are a lot more factors that influence the economic costs, for example, sea level rise, agriculture and human health. A more realistic cost function could probably be designed based on Stern (2007) but is beyond the scope of this study.~~

Due to these shortcomings, one cannot attribute much importance to the precise PNR values obtained for the PLASIM model ~~.~~ as in Fig. 7. However, we think that our approach is general enough for handling many different political and socio-economical ~~scenario's~~ scenarios combined with state-of-the-art climate models when the necessary simulations have been done with CMIP5 models to determine the Green's function, using LRT. Hence, it will be possible to make better estimates of the PNR for the real climate system. We therefore hope that eventually these ideas on the point of no return in climate change will become part of the decision-making process during future debates about climate change.

Acknowledgements. This study was supported by the MC-ETN CRITICS project. We thank Valerio Lucarini and Frank Lunkeit (Univ. Hamburg) to provide the PLASIM model data. We thank both reviewers, in particular K. Rypdal, for the excellent and stimulating comments which improved the paper substantially.

References

Aubin, J.-P.: Viability theory, Springer Science & Business Media, 2009.

Budyko, M.: Effect of solar radiation variation on climate of Earth, Tellus, 21, 611–619, 1969.

Doyen, L. and De Lara, M.: Stochastic viability and dynamic programming, Systems & Control Letters, 59, 629–634, 2010.

Edenhofer, O., Knopf, B., Barker, T., Baumstark, L., Bellevrat, E., Chateau, B., Criqui, P., Isaac, M., Kitous, A., Kypreos, S., et al.: The economics of low stabilization: model comparison of mitigation strategies and costs, The Energy Journal, pp. 11–48, 2010.

Fraedrich, K., Jansen, H., Kirk, E., Luksch, U., and Lunkeit, F.: The Planet Simulator: Towards a user friendly model, Meteorologische Zeitschrift, 14, 299–304, 2005.

Hansen, J., Sato, M., Kharecha, P., Beerling, D., Berner, R., Masson-Delmotte, V., Pagani, M., Raymo, M., Royer, D. L., and Zachos, J. C.: Target atmospheric CO2: Where should humanity aim?, arXiv preprint arXiv:0804.1126, 2008.

Heitzig, J., Kittel, T., Donges, J. F., and Molkenthin, N.: Topology of sustainable management of dynamical systems with desirable states: from defining planetary boundaries to safe operating spaces in the Earth system, Earth System Dynamics, 7, 21–50, 2016.

Hogg, A. M.: Glacial cycles and carbon dioxide: A conceptual model, Geophysical research letters, 35, 2008.

Joos, F., Roth, R., Fuglestvedt, J. S., Peters, G. P., Enting, I. G., von Bloh, W., Brovkin, V., Burke, E. J., Eby, M., Edwards, N. R., Friedrich, T., Frölicher, T. L., Halloran, P. R., Holden, P. B., Jones, C., Kleinen, T., Mackenzie, F. T., Matsumoto, K., Meinshausen, M., Plattner, G.-K., Reisinger, A., Segschneider, J., Shaffer, G., Steinacher, M., Strassmann, K., Tanaka, K., Timmermann, A., and Weaver, A. J.: Carbon dioxide and climate impulse response functions for the computation of greenhouse gas metrics: a multi-model analysis, Atmospheric Chemistry and Physics, 13, 2793–2825, doi:10.5194/acp-13-2793-2013, http://www.atmos-chem-phys.net/13/2793/2013/, 2013.

Mann, M. E.: Defining dangerous anthropogenic interference, Proceedings of the National Academy of Sciences, 106, 4065–4066, 2009.

Meinshausen, M., Smith, S. J., Calvin, K., Daniel, J. S., Kainuma, M. L. T., Lamarque, J.-F., Matsumoto, K., Montzka, S. A., Raper, S. C. B., Riahi, K., Thomson, A., Velders, G. J. M., and van Vuuren, D. P.: The RCP greenhouse gas concentrations and their extensions from 1765 to 2300, Climatic Change, 109, 213–241, doi:10.1007/s10584-011-0156-z, http://link.springer.com/10.1007/s10584-011-0156-z, 2011.

Myhre, G., Shindell, D., Bréon, F.-M., Collins, W., Fuglestvedt, J., Huang, J., Koch, D., Lamarque, J.-F., Lee, D., Mendoza, B., Nakajima, T., Robock, A., Stephens, T., Takemura, T., and Zhang, H.: Anthropogenic and Natural Radiative Forcing Supplementary Material, in: Climate Change 2013 - The Physical Science Basis, edited by Change, I. P. o. C., chap. 8, Cambridge University Press, Cambridge, 2013.

Pachauri, R. K., Allen, M., Barros, V., Broome, J., Cramer, W., Christ, R., Church, J., Clarke, L., Dahe, Q., Dasgupta, P., et al.: Climate Change 2014: Synthesis Report. Contribution of Working Groups I, II and III to the Fifth Assessment Report of the Intergovernmental Panel on Climate Change, 2014.

Petschel-Held, G., Schellnhuber, H. J., Bruckner, T., Tóth, F. L., and Hasselmann, K.: The Tolerable Windows Approach: Theoretical and Methodological Foundations, Climatic Change, 41, 303–331, 1999.

Ragone, F., Lucarini, V., and Lunkeit, F.: A new framework for climate sensitivity and prediction: a modelling perspective, arXiv preprint arXiv:1403.4908, 2014.

Rogelj, J., Hare, W., Lowe, J., van Vuuren, D. P., Riahi, K., Matthews, B., Hanaoka, T., Jiang, K., and Meinshausen, M.: Emission pathways consistent with a 2°C global temperature limit, Nature Publishing Group, 1, 413–418, 2011.

Rypdal, K.: Global warming projections derived from an observation-based minimal model, Earth System Dynamics, 7, 51–70, doi:10.5194/esd-7-51-2016, http://www.earth-syst-dynam.net/7/51/2016/, 2016.

Sellers, W. D.: A global climatic model based on the energy balance of the earth-atmosphere system, Journal of Applied Meteorology, 8, 392–400, 1969.

Smith, J. B. and Schneider, S. H.: Assessing dangerous climate change through an update of the Intergovernmental Panel on Climate Change (IPCC)"reasons for concern", in: Proceedings of the National Academy of Sciences, 2009.

Stern, N.: The economics of climate change: the Stern review, cambridge University press, 2007.

Victor, D. G. and Kennel, C. F.: Climate policy: Ditch the 2 C warming goal, Nature, 514, 2014.